

Growth of Orthorhombic Tl-2201 Single Crystals by the Self-Flux Method

D.C. Peets,¹ Ruixing Liang,¹ D.A. Bonn,¹ W.N. Hardy,¹ and M. Raudsepp²

¹*Department of Physics and Astronomy, University of British Columbia,
6224 Agricultural Road, Vancouver, BC, Canada V6T 1Z1*

²*Department of Earth and Ocean Sciences, University of British Columbia,
6339 Stores Road, Vancouver, BC, Canada, V6T 1Z4*

(Dated: November 1, 2002)

Millimetre-sized single crystals of $Tl_2Ba_2CuO_{6+x}$ with T_c 's ranging from 5K to 90K have been grown using a copper-rich self-flux method. The crystals were found by X-ray diffraction to be orthorhombic for lower T_c 's, and tetragonal closer to optimal doping, consistent with the orthorhombic distortion being caused by the ordering of excess oxygen in the O(4) interstitial site. Lattice parameters have been determined for several dopings, and are in good agreement with earlier work on ceramics. These are the first orthorhombic single crystals ever reported of Tl-2201.

PACS numbers: 74.72.Fq, 81.10.Fq, 61.10.Nz, 74.25.Ha

Keywords: A1. Characterization, A1. X-ray diffraction, A2. Growth from melt, A2. Single crystal growth, B1. Cuprates, B2. Oxide superconducting materials

1. INTRODUCTION

In the underdoped and optimally doped regions of the high- T_c cuprates' phase diagram, very high quality $YBa_2Cu_3O_{7-x}$ (YBCO) crystals may be readily grown [1, 2], as may crystals of many other such superconductors. In contrast to this situation, only a handful of compounds are known which can be overdoped to any significant degree, and crystals of these have not been available with the same quality as the underdoped compounds. As a result, the overdoped regime remains poorly studied, although it is of great interest. In particular, hints of Fermi liquid-like behaviour [3, 4] suggest we may be able to understand the state from which superconductivity develops on this side of the phase diagram.

$Tl_2Ba_2CuO_{6+x}$ (Tl-2201), one of only a handful of high- T_c cuprates which may be heavily overdoped, exists in two chemically distinct phases, one orthorhombic and one tetragonal. The former has the stoichiometric formula $Tl_2Ba_2CuO_{6+x}$, and has a rhombic CuO_2 plaquette instead of square, associated with a splitting of the thallium sites along the orthorhombic (1 0 0) (tetragonal (1 1 0)) direction [5]. This splitting is likely caused, in turn, by the ordering of excess oxygen atoms in O(4) interstitial sites [6, 7, 8] in the Tl_2O_2 double layer. The tetragonal version is non-stoichiometric, having the chemical formula $Tl_{1.85}Ba_2Cu_{1.15}O_{6+x}$ { 5-8% of the Tl is replaced by Cu [5, 9]. The disorder introduced through cation substitution disrupts the oxygen ordering, driving the structure tetragonal. Because orthorhombicity is associated with lower disorder, the orthorhombic phase is preferred for fundamental research, but no crystals of this phase have previously been reported.

The major difficulties encountered in the Tl-Ba-Cu-O

system are the high toxicity and volatility of thallium oxides [10]. Once these issues have been dealt with, crystals of Tl-2201 may be readily grown by both KCl flux [11] and self-flux [8, 9, 12, 13] methods. Because KCl flux techniques have the potential to contaminate the crystals with alkalis, the growth of high-purity crystals requires that the self-flux method be employed.

To control thallium oxide evaporation, Hasegawa [12] sealed his reactants ($TlBaCu = 1:1.25:1$) inside a gold crucible in a steel or alumina bomb, and cooled them through the peritectic point at $0.7\frac{C}{h}$. Kolesnikov [8] loaded roughly 100 g of his starting mixture ($TlBaCu = 1:1:1$) into a YSZ crucible, then cooled it through the peritectic point at $4\frac{C}{h}$. His crystals grew in cubic-centimetre voids in the ingot. These were likely bubbles of vapour prevented from escaping by the large quantity of viscous material on top. The crystals were separated mechanically from the ingot in each case. We elected to use compositions near $TlBaCu = 1:1:1$, midway along the Tl-2201 liquidus line in the quasi-binary $Tl_2Ba_2O_5$ { CuO phase diagram [14]. This phase diagram exhibits a liquidus curve between 55% and 72% CuO where Tl-2201 is the primary phase.

Because $BaCO_3$ has the potential to form oxycarbonates, of which a significant number have been isolated (see for example [15]), it is essential that a CO_2 -free barium source be employed. BaO_2 , commonly used in the preparation of Tl-2201, is only available in technical grade (95%) and contains such impurities as iron, calcium and alkalis. In the present work, $BaCuO_2$ was used.

Alumina [9, 13, 16, 17] and gold [12, 18, 19] have been the most commonly-used crucible materials in this system. While Al^{3+} is extremely harmful to $YBa_2Cu_3O_{7-x}$, where it replaces Cu in the chains, Tl-2201 has no analogous sites. In fact, no Al was detected in crystals grown in alumina crucibles [9]. Gold is also not believed capable of infiltrating Tl-2201. Sealing, when attempted, was always with Au, which softens at growth temperatures for

Electronic address: dpeets@physics.ubc.ca; URL: <http://www.physics.ubc.ca/~supercon>

better sealing. We chose Al_2O_3 crucibles and Au seals.

2. CRYSTAL GROWTH

Preursor BaCuO_2 powder was prepared via solid state reaction from BaCO_3 (Aldrich-APL, 99.999% pure) and CuO (Alfa Aesar, 99.995%) by repeated calcining at 870 C under 1 atm flowing oxygen with intervening grinding. This powder was intimately mixed with Tl_2O_3 (Alfa Aesar, 99.99% pure), and 15–20 g of the mixture were packed into a 10 mL alumina crucible. The crucible was sealed as depicted schematically in Fig. 1.

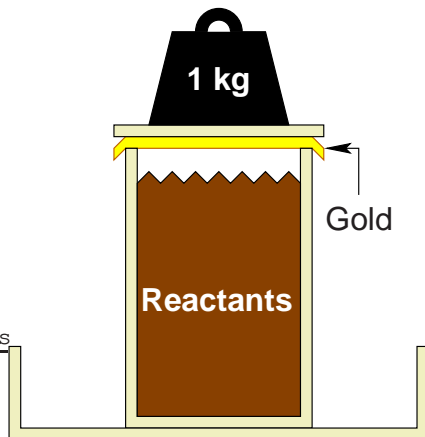


FIG. 1: Schematic diagram of growth setup, including powder charge, gold seal, weight, and alumina crucible, lid and tray.

To aid in sealing, a 1 kg weight was placed atop the crucible's lid. While O_2 gas may still escape as the Tl_2O_3 decomposes, the seal becomes very effective once the contents of the crucible equilibrate at the growth temperature. A typical growth with initial composition $\text{TlBaCu} = 1:1:1$ lost 6% of its thallium over the course of 56 h at growth temperatures, prompting an adjustment of the starting composition to 1.05:1:1. The effectiveness of the weight-assisted sealing was further demonstrated when the temperature was held at 550 C for several hours during cooling (the gold disc was deformed severely by the reduced pressure in the crucible).

Growth was performed in a horizontal tube furnace under flowing oxygen, with the crucible supported by a rectangular alumina tray at the centre of the heated zone. Temperature was controlled using a Platine-HI thermocouple which had been calibrated against a factory-calibrated R-type thermocouple. The exhaust gas was bubbled through 1.8 M H_2SO_4 to remove any thallium, but most of the escaped thallium precipitated out on the wall of the furnace tube upon leaving the heated zone.

The charge was heated rapidly ($300\frac{\text{C}}{\text{h}}$) to 935 C, and held for $\frac{1}{2}$ h to equilibrate. It was cooled at $\frac{1}{2}\frac{\text{C}}{\text{h}}$ to 890 C, then allowed to cool freely to room temperature. Crystals were extracted mechanically from the solidified

ingot of flux, then annealed under controlled oxygen partial pressures between 10^{-5} and 10^{-7} atm at temperatures between 290 C and 500 C. The results obtained were consistent with the relationship between temperature, oxygen partial pressure and T_c reported in [20]. A comprehensive investigation of oxygen annealing in this system is currently underway.

3. CHARACTERIZATION

Most crystals were embedded in flux, but free-standing crystals were found in voids inside the ingots; these were thin platelets with areas up to 1.2 mm^2 , with mirror surfaces and with fine curved growth steps visible. Several such crystals are shown in Fig. 2. Larger crystals, up to $5\text{ mm} \times 5\text{ mm} \times 0.5\text{ mm}$, were coated in flux. No apparent corrosion of the gold lid or alumina crucible was observed.

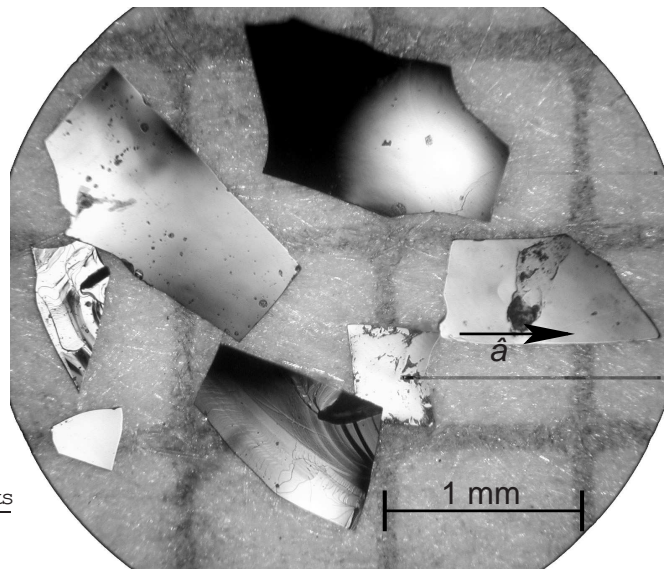


FIG. 2: Optical micrograph of several orthorhombic $\text{Tl}_2\text{Ba}_2\text{CuO}_{6+}$ crystals ($T_c = 24\text{K}$, annealing condition A below), resting on mm-ruled graph paper for scale. The orthorhombic a -axis of one crystal is indicated.

As-grown crystals typically exhibited T_c 's of 5–10K, several Kelvin wide, with a handful of crystals exhibiting T_c 's as high as 90K. In attempts to obtain homogeneous oxygen contents, crystals were annealed under two different conditions: A) 290C, $P_{\text{O}_2} = 10^{-9}$ atm for 14 days, and B) 430 C, $P_{\text{O}_2} = 10^{-10}$ atm for 6 days.

Magnetization measurements were performed in fields of several Tesla (HkC, in a Quantum Design SQUID magnetometer (MPMS)). Fig. 3 shows the field-cooled magnetization, measured at 2 Oe, of two crystals. The transition widths (10%–90%) of crystals annealed in conditions A and B were 4K and 0.7K respectively, which are significantly better than the widths of 5–10K reported

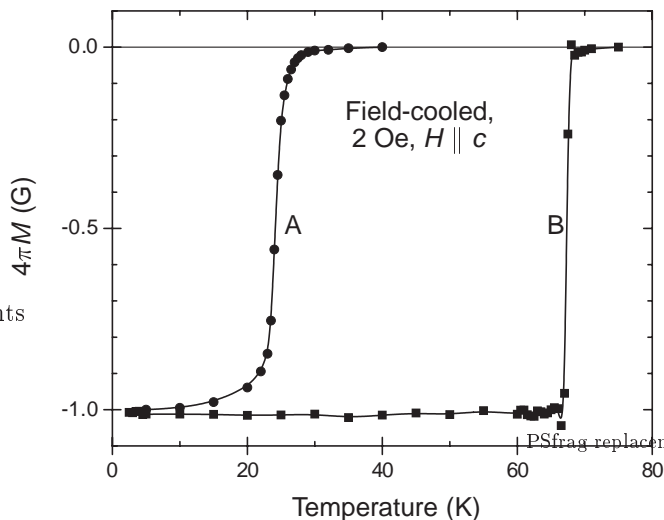


FIG. 3: Field-cooled magnetization curves for crystals annealed in conditions A and B. Condition A (○) yields crystals with $T_c = 24\text{K}$ and condition B (□) $T_c = 67.7\text{K}$.

on annealed ceramics [5, 20]. The observed Meissner fraction (fraction of flux excluded when cooling through T_c) of 40–60% compares well with field-cooled results on other cuprate superconductors. This compound's extremely low critical field H_{c1} made the transitions appear broader in higher applied fields.

To investigate the samples' crystallinity, X-ray diffraction (XRD) spectra were taken using $\text{CuK}\alpha_1$ radiation and a BEDE model 200 double-crystal diffractometer with a $\text{Si}(111)$ monochromator. The X-ray beam was sufficiently wide as to irradiate the entire crystal. The X-ray study concentrated on void-grown crystals, and found them to be orthorhombic as grown. Crystals annealed in condition A had lattice parameters $a = 5.4580(3)\text{Å}$, $b = 5.4848(5)\text{Å}$ and $c = 23.2014(5)\text{Å}$. Crystals annealed in condition B were tetragonal with lattice parameters $a = 3.8647(4)\text{Å}$ and $c = 23.247(1)\text{Å}$. At this oxygen doping, it appears that there are no longer enough interstitial oxygen atoms present to keep the crystals orthorhombic. These results are in qualitative agreement with earlier work on ceramics [5, 20]. Larger, flux-encrusted crystals had poor crystallinity and were found to be tetragonal at all dopings.

Fig. 4 depicts the (0 0 10) X-ray rocking curve of a $0.5 \times 1.2\text{ mm}$ crystal annealed under condition B ($T_c = 67.7\text{K}$). The FWHM of 0.034 is wider than the 0.006 obtained for the best $\text{YBa}_2\text{Cu}_3\text{O}_{7-x}$ crystals grown in BaZrO_3 crucibles, but is similar to the 0.02–0.03 achieved for $\text{YBa}_2\text{Cu}_3\text{O}_{7-x}$ grown in YSZ crucibles. This indicates a high degree of crystalline perfection.

Electron-probe micro-analyses (EPMA) of $\text{Tl}_2\text{Ba}_2\text{CuO}_{6+}$ crystals were performed on a fully-automated CAMECA SX-50 instrument, operating in wavelength-dispersion mode with the following operating

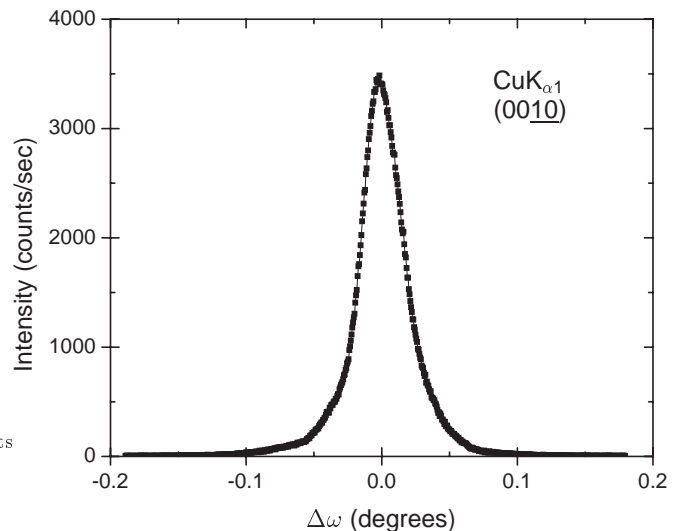


FIG. 4: (0 0 10) rocking curve for a typical crystal ($T_c = 67.7\text{K}$): the FWHM is 0.034°.

conditions: excitation voltage, 15 kV; beam current, 20 nA; peak count time, 80 s; background count time, 40 s; spot diameter, 10 mm. Data reduction was done using the "PAP" (Z) method [21]. For the elements studied, the following standards, X-ray lines and monochromator crystals were used: elemental Tl, Tm, PET; $\text{YBa}_2\text{Cu}_3\text{O}_{6.920}$, BaL, PET; $\text{YBa}_2\text{Cu}_3\text{O}_{6.920}$, $\text{CuK}\alpha_1$, LIF; and $\text{YBa}_2\text{Cu}_3\text{O}_{6.92}$, OK, W/Si. Tight Pulse Height Analysis (PHA) control was used to eliminate as much as possible any interference from higher-order X-ray lines.

In a study on two large, tetragonal crystals, the composition (normalized to barium) was found to be $\text{Tl}_{1.88(1)}\text{Ba}_2\text{Cu}_{1.11(2)}\text{O}_{6.6(1)}$ and homogeneous. Results on an orthorhombic crystal annealed in condition A were not significantly different. In terms of cation substitution, this composition is within error of previous work on the non-stoichiometric phase [5, 7, 9, 16]. Our anomalously high oxygen result is believed to be due to poorly-characterized mass absorption corrections in this system.

A check for trace Al contamination in the crystals was performed separately with the following operating conditions: excitation voltage, 15 kV; beam current, 40 nA; peak count time, 500 s; background count time, 250 s; spot diameter, 10 mm. The matrix composition was fixed at the nominal value for $\text{Tl}_2\text{Ba}_2\text{CuO}_{6+}$; AlK was standardized on Al_2O_3 using a TAP crystal monochromator. The aluminum concentration was found to be below the 50 ppm detection limit, corroborating the earlier observations that the crucibles were not corroded.

4. CONCLUSION

We have grown, annealed and characterized mm-sized orthorhombic single crystals of $\text{Tl}_2\text{2201}$. Their lattice pa-

rameters were found to be in qualitative agreement with earlier data on ceramic samples. The crystals' improved homogeneity was demonstrated by superconducting transitions nearly an order of magnitude narrower than has been reported for this compound, and their high crystalline perfection was indicated by a sharp X-ray rocking curve ($\text{FWHM} = 0.034$).

While the EPMA results show substitution of Tl by Cu, the orthorhombic symmetry of the crystals suggests the stoichiometric composition. The fact that crystals of both symmetries were obtained suggests that the composition of the crystals is near a boundary between the two phases.

The very effective sealing of the crucibles and resulting stability in growth conditions will enable a more thorough study of the Tl-Ba-Cu oxide phase diagram, permitting further optimization of the crystal growth technique. A comprehensive study of oxygen annealing conditions in

this system is also required. Work is commencing on both fronts.

The crystals grown in this study offer an opportunity for characterization of the overdoped regime by experiments that require clean samples, such as de Haas-van Alphen and Shubnikov-de Haas oscillations and microwave surface impedance measurements.

Acknowledgments

The authors wish to thank the Natural Sciences and Engineering Research Council of Canada and the Canadian Institute for Advanced Research for their support and D.M. Broun and A.P. Mackenzie for helpful discussions.

-
- [1] A. Erb, E. Walker, and R. Flükiger, *Physica C* 245, 245 (1995).
- [2] R. Liang, D.A. Bonn, and W.N. Hardy, *Physica C* 304, 105 (1998).
- [3] A.P. Mackenzie, S.R. Julian, D.C. Sinclair, and C.T. Lin, *Phys. Rev. B* 53, 5848 (1996).
- [4] A. Kaminski et al., 2002, condmat/0210531.
- [5] Y. Shimakawa, *Physica C* 204, 247 (1993).
- [6] J. B. Parise, C. C. Torardi, M. A. Subramanian, J. Gopalakrishnan, and A. W. Sleight, *Physica C* 159, 239 (1989).
- [7] Y. Shimakawa, Y. Kubo, T. Manako, and H. Igarashi, *Phys. Rev. B* 42, 10165 (1990).
- [8] N.N. Kolesnikov et al., *Physica C* 242, 385 (1995).
- [9] A. Tyler, An Investigation into the Magnetotransport Properties of Layered Superconducting Perovskites, Ph.D. thesis, University of Cambridge, 1998.
- [10] M.P. Siegal, E.L. Venturini, B.M. Rosin, and T.L. Aselage, *J. Mater. Res.* 12, 2825 (1997).
- [11] T. Manako, Y. Kubo, and Y. Shimakawa, *Phys. Rev. B* 46, 11019 (1992).
- [12] M. Hasegawa, H. Takei, K. Izawa, and Y. Matsuda, *J. Cryst. Growth* 229, 401 (2001).
- [13] N.N. Kolesnikov et al., *Physica C* 195, 219 (1992).
- [14] J.L. Jordan et al., *Physica C* 205, 177 (1993).
- [15] B. Raveau, C. Michel, B. Mercey, J.F. Hamet, and M. Hervieu, *J. Alloy Compd.* 229, 134 (1995).
- [16] R.S. Liu et al., *Physica C* 198, 203 (1992).
- [17] O.M. Vyasilev, N.N. Kolesnikov, M.P. Kulakov, and I.F. Schegolev, *Physica C* 199, 50 (1992).
- [18] C.C. Torardi et al., *Phys. Rev. B* 38, 225 (1988).
- [19] M. Hasegawa, Y. Matsushita, Y. Iye, and H. Takei, *Physica C* 231, 161 (1994).
- [20] C. Opagiste et al., *Physica C* 213, 17 (1993).
- [21] J.L. Pouchou and F. Pichoir, *Microbeam Analysis*, 104 (1985).